488   sulfate particles. *J. Aerosol Sci*. 40: 338–347.

489   Boselli, A., Caggiano R., Cornacchia C., Madonna F., Macchiato M., Mona L., Pappalardo G.,

490   Trippetta S. (2012). Multi year sun-photometer measurements for aerosol characterization in a

491   Central Mediterranean site. (2012). *Atmos. Res*. 104-105: 98-110.

492   Brogniez C., Lenoble J., Shaw G. (2013). Direct observation of the sun for aerosol retrieval. In:

493   *Aerosol Remote Sensing*. Lenoble J., Remer L., Tanre D. (eds) Springer, Berlin, Heidelberg.

494   Broomandi, P., Karaca, F., Nikfal, A., Jahanbakhshi, A., Tamjidi, M. and Kim, J.R. (2020).

495   Impact of COVID-19 Event on the Air Quality in Iran. *Aerosol Air Qual. Res.* 20: 1793–1804.

496   https://doi.org/10.4209/aaqr.2020.05.0205

497   Chameides, W.L., Fehsenfeld, F., Rodgers, M.O., Cardelino, C., Martinez, J., Parrish, D.,

498   Lonneman, W., Lawson, D.R., Rasmussen, R.A., Zimmerman, P., Greenberg, J., Middleton, P.,

499   Wang, T. (1992). Ozone precursor relationships in the ambient atmosphere. *J. Geophys. Res*.

500   97: 6037-6055. doi:10.1029/91JD03014

501   Dinoi, M., Conte, M., Grasso, F.M., Contini, D. (2020). Long-Term Characterization of

502   Submicron Atmospheric Particles in an Urban Background Site in Southern Italy. *Atmosphere*

503   11:334-349. doi:10.3390/atmos11040334

504   Dubovik, O. and King, M.D. (2000). A flexible inversion algorithm for the retrieval of aerosol

505   optical properties from sun and sky radiance measurements. *J. Geophys. Res*. 105: 20,673–

506   20,696. doi:10.1029/2000JD900282

507   EU Copernicus Program - European Air Quality information in support of the COVID-19 Crisis,

508   Inst. Web Site. (2020). https://atmosphere.copernicus.eu

509   Faridi, S., Yousefian, F., Niazi, S., Ghalhari, M.R., Hassanvand, M.S. and Naddafi, K. (2020).

510   Impact of SARS-CoV-2 on Ambient Air Particulate Matter in Tehran. *Aerosol Air Qual. Res.*

511   20: 1805–1811. https://doi.org/10.4209/aaqr.2020.05.0225

512   Filonchyk, M., Hurynovich, V., Yan, H., Gusev, A. and Shpilevskaya, N. (2020). Impact

513   Assessment of COVID-19 on Variations of SO2, NO2, CO and AOD over East China. *Aerosol*

514   *Air Qual. Res.* 20: 1530–1540. https://doi.org/10.4209/aaqr.2020.05.0226

515   Fotiadi, A., Hatzianastassiou, N., Drakakis, E., Matsoukas, C., Pavlakis, K.G., Hatzidimitriou, D.,

516   Gerasopoulos, E., Mihalopoulos, N. and Vardavas I. Aerosol physical and optical properties in

517   the Eastern Mediterranean Basin, Crete, from Aerosol Robotic Network data. (2006) Atmos.

518   Chem. Phys., 6, 5399–5413, www.atmos-chem-phys.net/6/5399/2006/

519   Giles, D. M., Sinyuk, A., Sorokin, M. G., Schafer, J. S., Smirnov, A., Slutsker, I., Eck, T. F.,

520   Holben, B. N., Lewis, J. R., Campbell, J. R., Welton, E. J., Korkin, S. V., Lyapustin, A. I.

521   (2019) Advancements in the Aerosol Robotic Network (AERONET) Version 3 database –

522   automated near-real-time quality control algorithm with improved cloud screening for Sun

523   photometer aerosol optical depth (AOD) measurements. *Atmos. Meas. Tech*. 12: 169–209.

524   https://doi.org/10.5194/amt-12-169-2019, 2019.

525   Holben, B.N., Eck, T.F., Slutsker, I., Tanré, D., Buis, J.P., Setzer, A., Vermote, E., Reagan, J.A.,

526   Kaufman, Y.J., Nakajima, T., Lavenu, F., Jankowiak, I.,Smirnov, A. (1998). AERONET—a

527   federated instrument network and data archive for aerosol characterization. *Remote. Sens.*

528   *Environ.* 66: 1–16.

529   Holben, B.N., Tanré, D., Smirnov, A., Eck, T.F., Slutsker, I., Abuhassan, N., Newcomb, W.W.,

530   Schafer, J., Chatenet, B., Lavenue, F., Kaufman, Y.J., Vande Castle, J., Setzer, A., Markham,

531   B., Clark, D., Frouin, R., Halthore, R., Karnieli, A., O'Neill, N.T., Pietras, C., Pinker, R.T.,

532   Voss, K., Zibordi, G. (2001). An emerging ground-based aerosol climatology: aerosol optical

533   depth from AERONET. *J. Geophys. Res*. 106: 12,067–12,097. doi:10.1029/ 2001JD900014

534   Kaskaoutis, D.G., Kambezidisa, H.D, Adamopoulosb, A.D., Kassomenos, P.A. (2006) On the

535   characterization of aerosols using the Å ngström exponent in the Athens area. *J. of Atmos. and*

536   *Solar-Terrestrial Phys.* 68: 2147–2163.

537   Liu, J., Zheng, Y., Li, Z., Flynn, C., Cribb, M. (2012). Seasonal variations of aerosol optical

538   properties, vertical distribution and associated radiative effects in the Yangtze Delta region of

539   China. „*J. Geophys. Res*.117. doi:10.1029/2011JD016490

540   Mahato S., Pal S., Ghosh K.G. (2020). Effect of lockdown amid COVID-19 pandemic on air

541   quality of the megacity Delhi, India. *Sci. Total Environ*. 730.

542   doi:10.1016/j.scitotenv.2020.139086

543   Mallet, M., Dulac, F., Formenti, P., Nabat, P., Sciare, J., Roberts, G., Pelon, J., Ancellet, G.,

544   Tanré, D., Parol, F., Denjean, C., Brogniez, G., di Sarra, A., Alados-Arboledas, L., Arndt, J.,

545   Auriol, F., Blarel, L., Bourrianne, T., Chazette, P., Chevaillier, S., Claeys, M., D'Anna, B.,

546   Derimian, Y., Desboeufs, K., Di Iorio, T., Doussin, J.-F., Durand, P., Féron, A., Freney, E.,

547   Gaimoz, C., Goloub, P., Gómez-Amo, J. L., Granados-Muñoz, M. J., Grand, N., Hamonou, E.,

548   Jankowiak, I., Jeannot, M., Léon, J.-F., Maillé, M., Mailler, S., Meloni, D., Menut, L.,

549   Momboisse, G., Nicolas, J., Podvin, T., Pont, V., Rea, G., Renard, J.-B., Roblou, L.,

550   Schepanski, K., Schwarzenboeck, A., Sellegri, K., Sicard, M., Solmon, F., Somot, S., Torres,

551   B., Totems, J., Triquet, S., Verdier, N., Verwaerde, C., Waquet, F., Wenger, J., and Zapf, P.

552   (2016). Overview of the Chemistry-Aerosol Mediterranean Experiment/Aerosol Direct

553   Radiative Forcing on the Mediterranean Climate (ChArMEx/ADRIMED) summer 2013

554   campaign. *Atmos. Chem. Phys*. 16: 455–504. https://doi.org/10.5194/acp-16-455-2016

555   Nakada, L.Y.K. and Urban, R.C. (2020). COVID-19 pandemic: Impacts on the air quality during

556   the partial lockdown in São Paulo state, Brazil. *Sci. Total Environ*. 730.

557   doi:10.1016/j.scitotenv.2020.139087

558   Pavese, G., Lettino, A, Calvello, M., Esposito, F., Fiore, S. (2016) Aerosol Composition and

559   Properties Variation at the Ground and Over the Column Under Different Air Masses

560   Advection in South Ital. *Environ Sci Pollut. Res Int*. 23: 6546-6562. doi: 10.1007/s11356-015-

561   5860-1.

562   Pisani, G., Boselli, A., Spinelli, N., Wang, X. (2011). Characterization of Saharan dust layers

563   over Naples (Italy) during 2000-2003 EARLINET project. *Atmos. Res*. 102: 286-299. doi:

564   10.1016/j.atmosres.2011.07.012

565   Reid, J.S., Eck, T.F., Christopher, S.A., Hobbs, P.V., Holben, B.N. (1999). Use of the Ångström

566   exponent to estimate the variability of optical and physical properties of aging smoke particles

567   in Brazil. *J. Geophys. Res*. 104: 27,473–27,489. doi:10.1029/1999JD900833

568   Sharma, S., Zhang, M., Anshika, Gao, J., Zhang, H., Kota, S.H. (2020). Effect of restricted

569   emissions during COVID-19 on air quality in India. *Sci. Total Environ*. 728.

570   doi:10.1016/j.scitotenv.2020.138878

571   Sicart, M., Barragan, R., Dulac, F., Alados-Arboledas, L., and Mallet, M. Aerosol optical,

572   microphysical and radiative properties at regional background insular sites in the western

573   Mediterranean. (2016) *Atmos. Chem. Phys.* 16: 12177–12203. doi:10.5194/acp-16-12177-2016

574   Sillman S. (1999). The relation between ozone, NO(x) and hydrocarbons in urban and polluted

575   rural environments. *Atmos. Environ*. 33: 1821–1845. doi:10.1016/S1352-2310(98)00345-8

576   Taylor J.R. (2018) *An introduction to error analysis*, 2nd Edition. University Science Books.

577   Sausalito.

578   Tobías, A., Carnerero, C., Reche, C., Massagué, J., Via, M., Minguillón, M.C., Alastuey, A.,

579   Querol, X. (2020). Changes in air quality during the lockdown in Barcelona (Spain) one month

580   into the SARS-CoV-2 epidemic. *Sci. Total Environ*. 726. doi:10.1016/j.scitotenv.2020.138540

581   Toledano, C., Cachorro, V.E., Berjon, A., de Frutos, A.M., Sorribas, M., de la Morena, B.A.,

582   Goloub, P. (2007). Aerosol optical depth and Ångström exponent climatology at El Arenosillo

583   AERONET site (Huelva,Spain). *Q.J. R. Meteorol. Soc*. 133: 795–807.

584   Tomasi, C., Fuzzi, S., Kokhanovsky, A. (eds.). (2016). *Atmospheric Aerosols - Life Cycles and*

585   *Effects on Air Quality and Climate*. Wiley-VCH Verlag GmbH & Co. Weinheim, Germany.

586   Valenzuela, A., Olmo, F.J., Lyamani, H., Granados-Muñoz, M. J., Antón, M., Guerrero-Rascado,

587   J.L., Quirantes, A., Toledano, C., Perez-Ramírez, D., Alados-Arboledas, L. (2014). Aerosol

588   transport over the western Mediterranean basin: Evidence of the contribution of fine particles

589   to desert dust plumes over Alborán Island. *J. Geophys .Res. Atmos*. 119: 14,028–14,044.

590   doi:10.1002/2014JD022044

591   www.arpacampania.it, Inst. Web Site. (2020).

592   Xu, K., Cui, K., Young, L.H., Y.K. Hsieh, Y.K., Wang, Y.F., Zhang, J. Wan, S. (2020a) Impact

593   of the COVID-19 Event on Air Quality in Central China. *Aerosol Air Qual. Res*. 20: 915–929.

594   doi:10.4209/aaqr.2020.04.0150

595   Xu, K., Cui, K., Young, L.H., Wang, Y.F., Hsieh, Y.K., Wan, S. and Zhang, J. (2020b). Air

596   Quality Index, Indicatory Air Pollutants and Impact of COVID-19 Event on the Air Quality

597   near   Central   China.   *Aerosol   Air   Qual.   Res.*   20:   1204–1221.

598   https://doi.org/10.4209/aaqr.2020.04.0139

599   Zambrano-Monserrate, M.A., Ruano, M.A., Sanchez-Alcalde, L., (2020). Indirect effects of

600   COVID-19 on the environment: *Sci. Total Environ*. 728. doi:10.1016/j.scitotenv.2020.138813

601

602

603

604 **Table 1.** Mean values of the PM concentration (μg m^{-3}) registered by sampling stations
605 located at the four reference city points (VP, AO, NM, AS) for the period preceding the
606 lockdown (P) and during the lockdown (L) for the year 2019.

Station	VP		AO		NM		AS	
Period (P/L)	P	L	P	L	P	L	P	L
PM$_{10}$	19±1	15±1	23±2	25±1	28±2	22±1	36±3	23±1
PM$_{2.5}$	12±1	9.4±0.7	13±1	16±3	18±1	11±1	26±3	13±1

607

608

609 **Table 2.** Mean values of the PM concentration ($\mu g\ m^{-3}$) registered by sampling stations
610 located at the four reference city points (VP, AO, NM, AS) and by the OPC at the university
611 campus (UC) for the period preceding the lockdown (P) and during the lockdown (L) for the
612 year 2020.

Station	VP		AO		NM		AS		UC	
Period (P/L)	P	L	P	L	P	L	P	L	P	L
PM_{10}	13±1	18±2	34±2	30±2	31±2	22±2	51±5	27±3	19±1	23±2
$PM_{2.5}$	7±1	12±1	17±2	15±1	21±2	15±2	37±4	19±2	14±1	17±2
PM_1	-		-		-		-		10.7±0.9	16±2

613

614

Table 3. Mean values of C_6H_6, CO and NO_2 concentration ($\mu g\ m^{-3}$) registered by sampling stations located at the four reference city points (VP, AO, NM, AS) and SO_2 ($\mu g\ m^{-3}$) for VP and AS in the period preceding the lockdown (P) and during the lockdown (L) phase for the years 2019 and 2020.

Station	VP		AO		NM		AS	
Period (P/L)	P	L	P	L	P	L	P	L
Year 2019								
C_6H_6	0.60±0.06	0.60±0.06	2.0±0.1	1.2±0.1	2.8±0.2	1.3±0.1	1.7±0.2	0.4±0.04
CO	0.50±0.03	0.30±0.02	0.60±0.02	0.50±0.01	0.90±0.06	0.70±0.03	1.00±0.06	0.80±0.02
NO_2	12±1	5.6±0.6	30±2	22±2	61±3	48±3	50±2	40±2
SO_2	1.9±0.1	1.0±0.1	-	-	-	-	4.7±0.5	4±1
Year 2020								
C_6H_6	0.6±0.3	0.40±0.06	1.0±0.1	0.60±0.06	1.4±0.1	0.30±0.05	1.4±0.2	0.6±0.1
CO	0.20±0.04	0.20±0.03	0.50±0.03	0.40±0.04	1.0±0.1	0.50±0.03	1.2±0.1	0.50±0.02
NO_2	10±1	5.1±0.5	26±2	10±2	51±2	26±3	45±2	22±2
SO_2	3±1	1.4±0.2	-	-	-	-	4.4±0.2	1.3±0.4

Period (P/L)	Saharan Dust				No Saharan Dust			
	Year 2019		Year 2020		Year 2019		Year 2020	
	P	L	P	L	P	L	P	L
	Solar							
AOD	0.18±0.01	0.22±0.01	0.27±0.09	0.26±0.04	0.12±0.01	0.18±0.02	0.19±0.01	0.24±0.04
	1.0±0.2	1.3±0.1	0.97±0.05	1.4±0.1	1.5±0.1	1.4±0.1	1.62±0.04	1.5±0.1
	Lunar							
AOD	0.3±0.1	0.3±0.1	0.21±0.03	0.29±0.07	0.18±0.04	0.19±0.02	0.17±0.02	0.34±0.03
	1.2±0.2	0.8±0.2	1.1±0.3	1.3±0.1	1.3±0.1	1.3±0.1	1.1±0.1	1.71±0.04

626

627

628   **Figure Captions**

629   **Fig. 1.** Map of the City of Naples with the indication of the location of the eight air sampling

630   stations and Optical Particles Counter at the University Campus. VP=Virgiliano Park;

631   ES=Epomeo Station; SH=Santobono Hospital; NM=National Museum; AO=Astronomic

632   Observatory; MRS=Main Railway Station; PH=Pellegrini Hospital; AS=Argine Street;

633   UC=University Campus. The four representative stations are reported in blue.

634   **Fig. 2.** Daily averaged values of the PM mass concentration ($\mu g\ m^{-3}$) monitored continuously by

635   the OPC from January 27th to April 30th, 2020. The shaded are tinted in light blue indicates the

636   lockdown period.

637   **Fig. 3.** AOD count distributions. Panels (a) and (b) report the histograms of solar data for the

638   Lockdown and Pre-lockdown periods, respectively. Panels (c) and (d) display the histograms of

639   lunar data for the Lockdown and Pre-lockdown periods, respectively.

640   **Fig. 4.** α count distributions. Panels (a) and (b) report the histograms of solar data for the

641   Lockdown and Pre-lockdown periods, respectively. Panels (c) and (d) display the histograms of

642   lunar data for the Lockdown and Pre-lockdown periods, respectively.

643   **Fig. 5.** α count distributions. Panels (a) and (b) report the histograms of solar data for the

644   Lockdown (black circles) and Pre-lockdown (yellow circles) periods, respectively. Panels (c) and

645   (d) display the histograms of lunar data for the Lockdown (black stars) and Pre-lockdown (blue

646   stars) periods, respectively.

647 **Fig. 6.** Columnar volume particle size distribution $dV(r)/dln(r)$ for year 2020 separated for the

648 cases without (panel (a) – NSD) and with the influence of Saharan dust (panel (b) – SD) events.

649 The two profiles in each panel refer to pre-lockdown (red circles) and lockdown (black squares)

650 respectively.

651

652

653

654
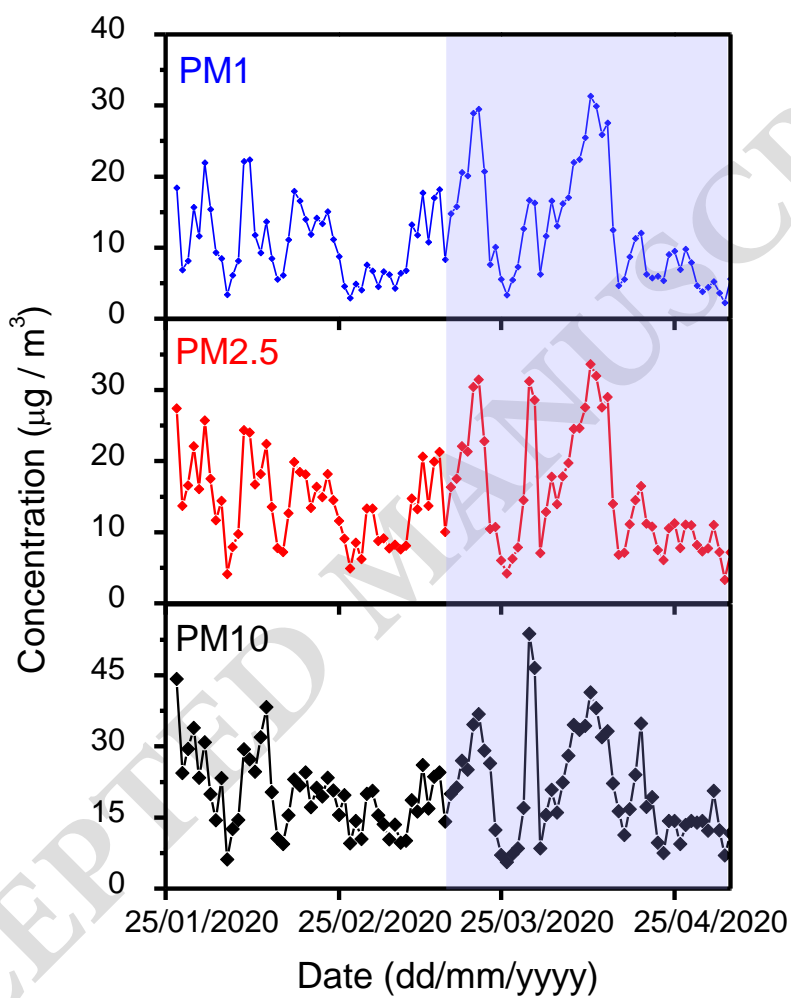
655

656

657

658

659

660

661

662   **Fig. 1.**

663

664

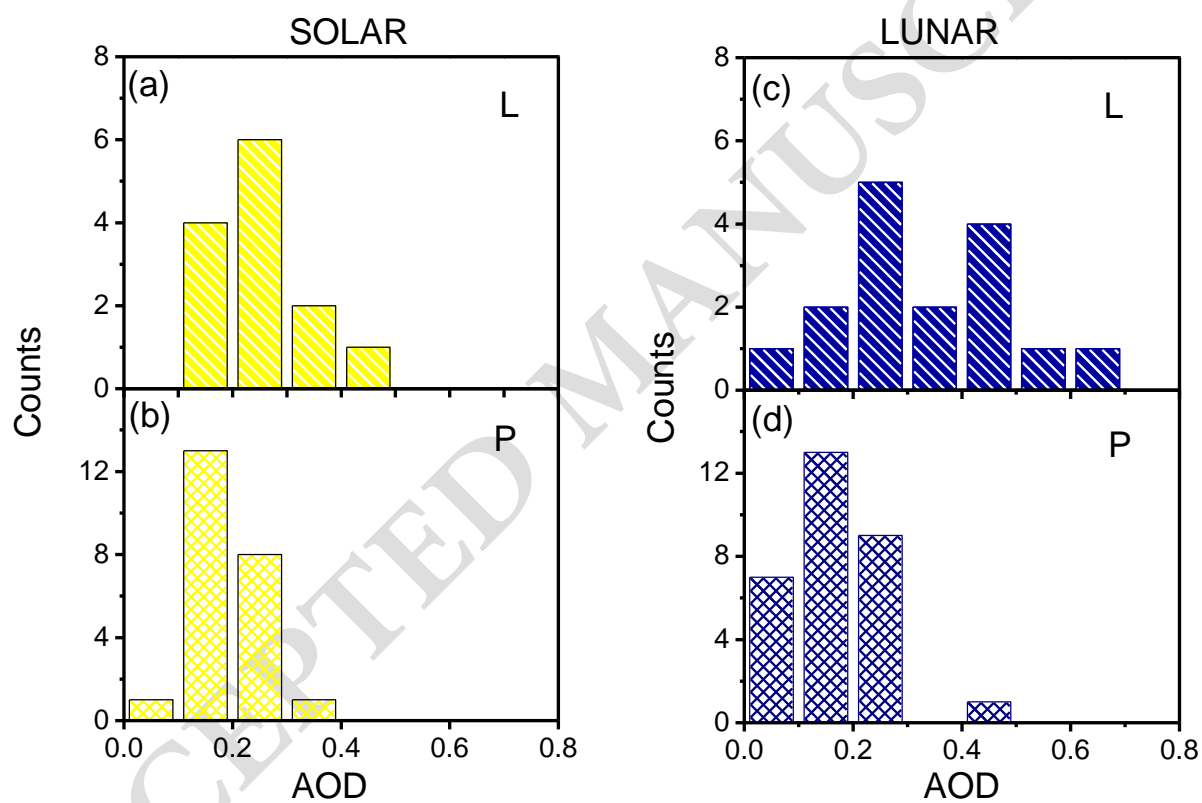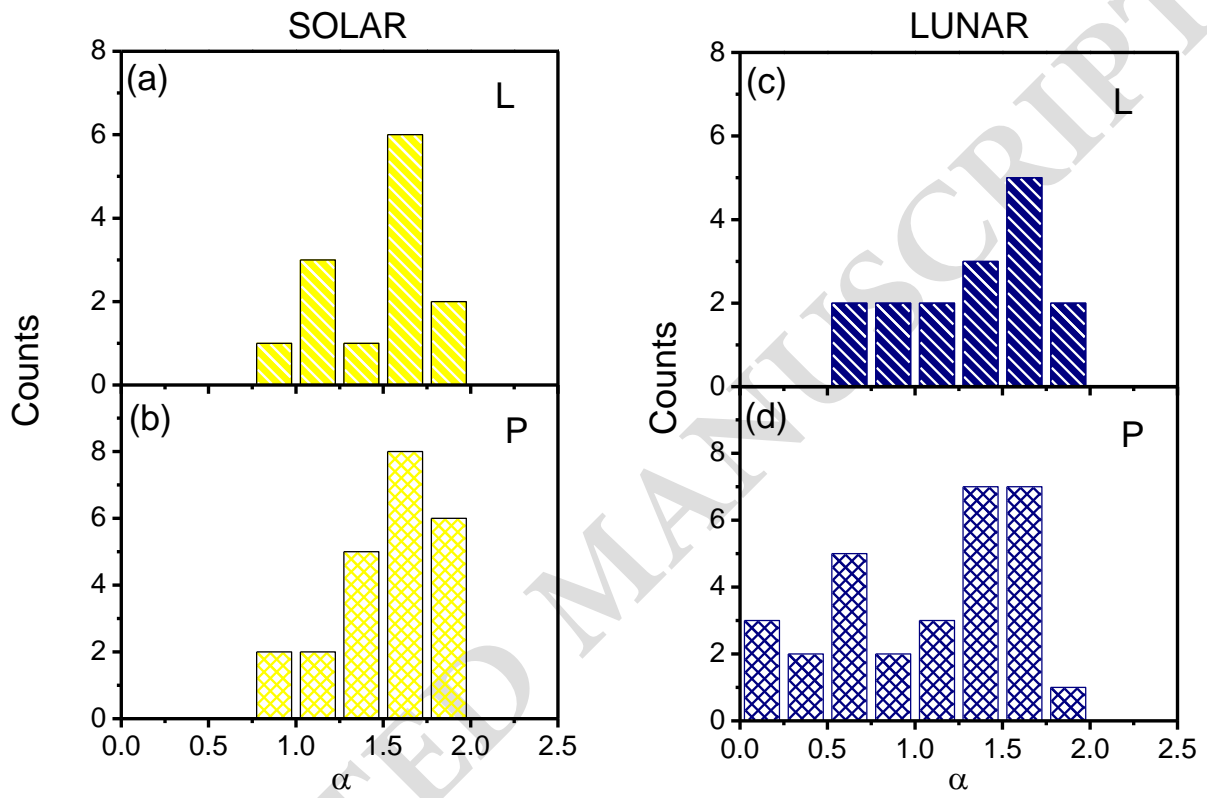665

666

667

668

669

670   **Fig. 2.**

671

672

673

674

675

676

677

SOLAR — (a) L, (b) P; **LUNAR** — (c) L, (d) P; Counts vs AOD

678

679

680

681

Fig. 3.

682

686
687

688

689

690   **Fig. 4.**

691
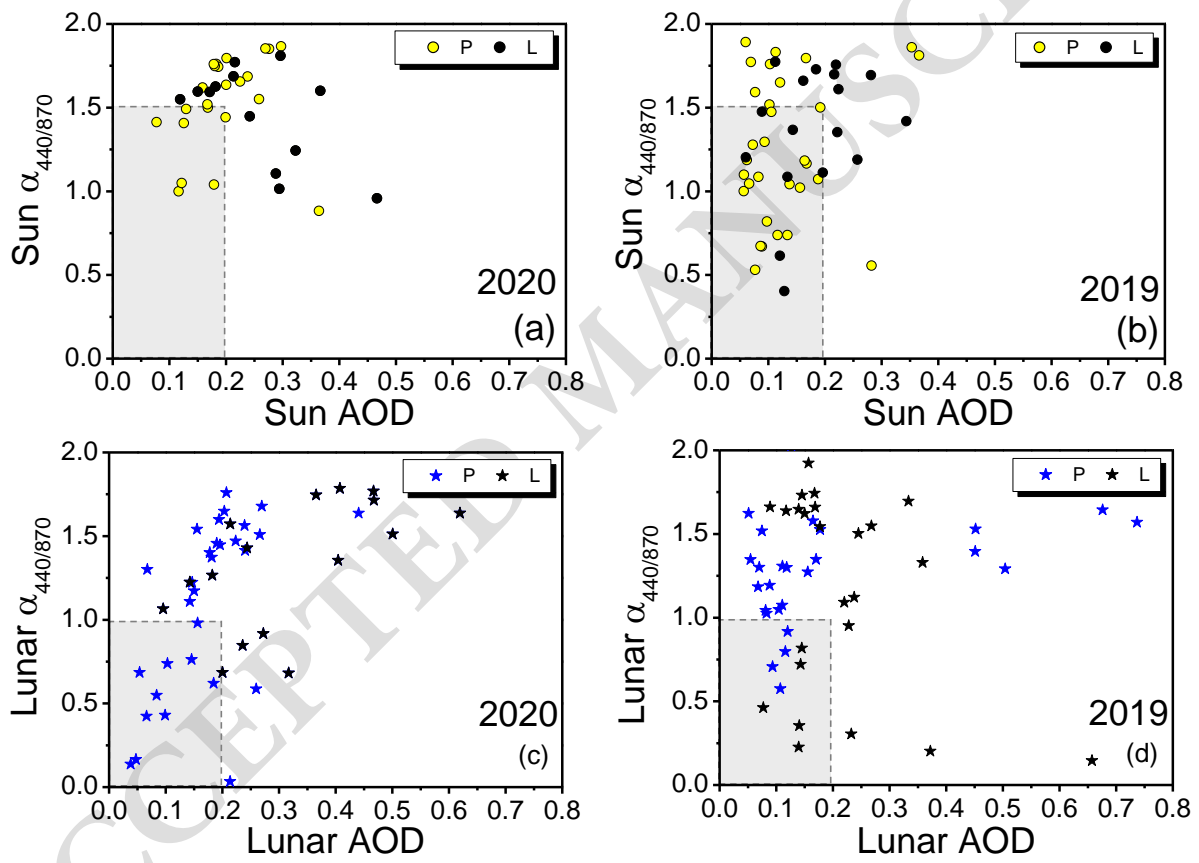
692

693

694

695

696

Fig. 5.

697

698

699

700

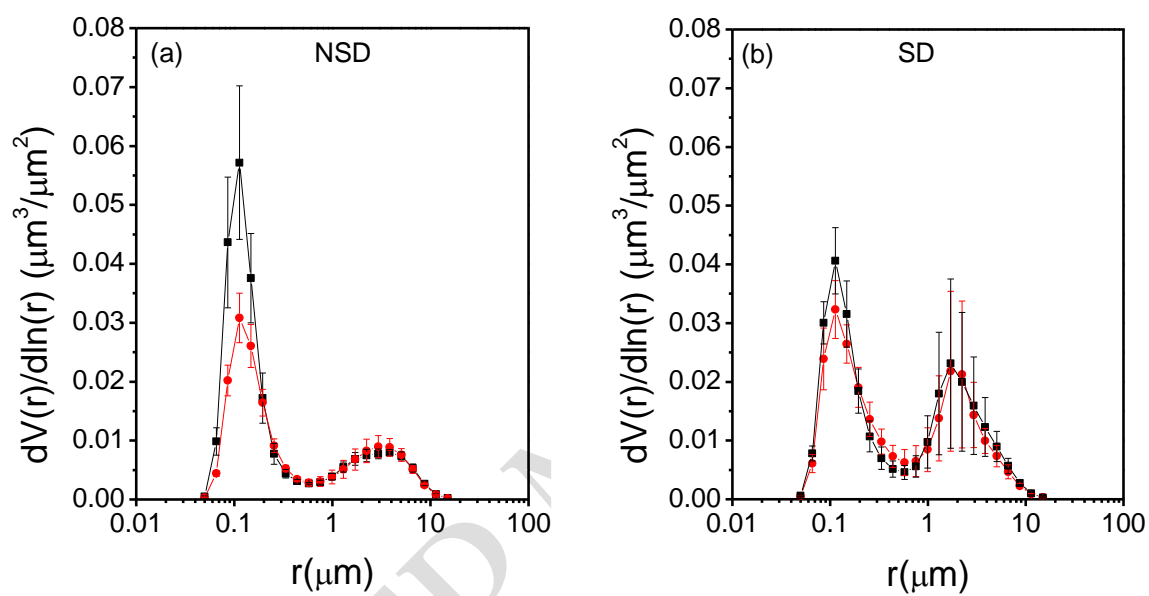701

702

703

704

705

706

707

708

709

710   **Fig. 6.**

711